Journal of Sound and Vibration (1997) **200**(3), 371–378

ANALYSIS AND COMPARISON OF THE DENSITY FUNCTIONS IN A CHAOTIC, SLEWING LINK

R. Stockton and E. Garcia

Department of Mechanical Engineering, Vanderbilt University, Nashville, Tennessee 37235, *U.S.A.*

(*Received* 15 *April* 1996)

1. INTRODUCTION

The modelling and control of flexible space structures is a topic of much current research. Some examples are the NASA Remote Manipulator System (RMS) on the Space Shuttle and appendages of satellites (e.g., solar panels). Typically, these structures are required to slew about a fixed or hinged location and are subsequently made rigid and massive to prohibit bending or torsion along any of their axes. In space-borne structures, size and mass are a significant factor wherein a less massive structure results in a lighter, faster mechanism and more economial operation and cost-effectiveness. The combination of low mass and long lengths results in a highly flexible structure with low natural frequencies.

If the vibrations from a lightweight, flexible, slewing link are chaotic, then precise prediction of the long term time history is impossible, while the near term history may be quite good. Small uncertainties in the initial conditions lead to diverging responses. A statistical measure of the chaotic dynamics can be obtained by using the probability density functions [1]. Measurement of the density functions (probability, PDF, and cumulative, CDF) can be used as a diagnostic tool especially in periodically forced systems. Probabilistic theory is capable of distinguishing different degrees of complexity of motions, and presents a further step in bridging the gap between simple systems and complicated dynamics.

This note will focus on the physically relevant case of a flexible link (a simple model of a robot manipulator arm) undergoing periodic slewing motion (as normally occurs in repetitious tasks). The equations of motion take into account Coriolis and centripetal forces as well as other non-linear terms. This system is known to undergo chaotic motion for certain parameters (e.g., initial deflection and amplitude of the forcing function) [2]. The amplitude PDF and CDF for the position and velocity, $P(y)$ and $P(\dot{y})$, of the system will be used as an identification technique for chaos in a probabilistic setting. The system is investigated for multi-maxima peaks typical of chaotic distributions. The chaotic distributions of the model are compared to the standard normal distribution. both the chi-squared and Kolmogorov–Smirnov goodness of fit tests are used.

2. EQUATIONS OF MOTION

The flexible, slewing link model consists of a beam with small moment of inertia attached to an actuating motor with a large gear ratio, allowing little or no interaction between the vibrations of the beam and the rotations of the motor (see Figure 1). The actuator is isolated from the beam's flexure and the actuator's inertia can be considered to be negligible. In a slewing manipulator, the inertial non-linearities are dominant over the geometric non-linearities, especially if a payload is involved. The use of a rotating

0022–460X/97/080371 + 08 $25.00/0/sv960644

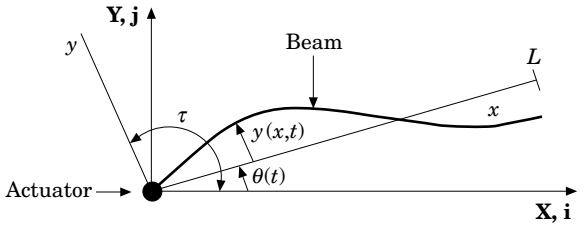

Figure 1. A schematic diagram of the rotating axis with an attached flexible link.

co-ordinate frame allows a simple expression for the total potential energy of the beam. In the derivation, the following conditions for the beam are applied: (1) cross-sections are assumed to remain plane and normal to the bending axis; (2) axial displacement, torsion, shear and gravity effects are negligible.

Consider the system shown in Figure 1: the position of any point along the link in terms of the inertial frame X–Y is given by $\mathbf{r} = (x\cos\theta - y\sin\theta)\hat{\mathbf{i}} + (x\sin\theta + y\cos\theta)\hat{\mathbf{j}}$. The magnitude of the velocity at any point on the link is obtained by taking the first time derivative of the position and finding the square, $\dot{\mathbf{r}}^2 = x^2\dot{\theta}^2 + 2x\dot{y}\dot{\theta} + y^2\dot{\theta}^2 + \dot{y}^2$. In the above, $\hat{\mathbf{i}}$ and $\hat{\mathbf{j}}$ are the unit vectors of the reference frame X and Y, respectively, $\theta = \theta(t)$ describes the hub angle between the rigid (non-flexible) link and the horizontal axis, and $y = y(x, t)$ describes the deviation of the link from the rigid case, where x is some value between 0 and L, and L is the total length of the beam.

The kinetic and potential energies of the beam, respectively, are

$$T = \tfrac{1}{2}\int_0^L \rho(x^2\dot{\theta}^2 + 2x\dot{y}\dot{\theta} + y^2\dot{\theta}^2 + \dot{y}^2)\,\mathrm{d}x, \qquad V = \tfrac{1}{2}\int_0^L EI(y'')^2\,\mathrm{d}x, \tag{1}$$

where T is found by multiplying the magnitude of the velocity of each differential mass element $\rho\,\mathrm{d}x$ and integrating over the entire length of the beam, ρ is the mass per unit length, E is Young's modulus for the beam, and I is the area moment of inertia of the link.

Using Lagrange's equation, applying Hamilton's principle (taking the first variation) and by repeated integration by parts, the dynamic equations of motion are derived. For simplicity, the non-conservative work, W_{nc}, is assumed to be $\tau\theta$, where τ is the applied torque and θ is the total angular deflection. The $\delta\theta$ terms describe the rigid body position of the beam and the δy terms describe the flexure of the beam along its length. The non-linearities result from Coriolis, centripetal acceleration and other non-linear terms:

$$\delta\theta, \quad \int_0^L \rho(x^2\ddot{\theta} + x\ddot{y} + y^2\ddot{\theta} + 2y\dot{y}\dot{\theta})\,\mathrm{d}x - \tau = 0; \tag{2}$$

$$\delta y, \quad \int_0^L [\rho(x\ddot{\theta} - \dot{\theta}^2 y + \ddot{y}) + EIy'''']\,\mathrm{d}x = 0. \tag{3}$$

The motion of the structure is now discretized by applying a modal summation procedure. The deflection $y(x, t)$ can be approximated by the expression,

$$y(x, t) = \sum_{i=1}^{n} \phi_i(x)q_i(t),$$

where the admissible basis functions (clamped–free) are defined by $\phi_i(x)$, and the time dependent modal co-ordinates are defined by $q_i(t)$. By taking the case in which $i = 1$, a two mode model is obtained, sufficient to display the interactions between the rigid body and the first bending mode during the slew of the structure.

By masking the following substitutions, where δ_{ij} is the Kroneker delta function:

$$\int_0^L \rho x^2 \ddot{\theta}\, \mathrm{d}x = I_b; \qquad \int_0^L \rho x \phi_i(x)\, \mathrm{d}x = I_i; \qquad \int_0^L \rho \phi_i(x)\phi_j(x)\, \mathrm{d}x = m_i\, \delta_{ij}, \tag{4}$$

and substituting $y(x, t)$ into equation (2), the equation for the rigid body position can then be represented by the non-linear equation

$$(I_b + m_1 q_1^2)\ddot{\theta} + I_1 \ddot{q}_1 + 2m_1 q_1 \dot{q}_1 \dot{\theta} + b_v \dot{\theta} = \tau = A \sin \omega_f t, \tag{5}$$

where the linear damping term $b_v\dot{\theta}$ has been added to model the damping between the slewing actuator and the flexible structure.

For the beam modes, substituting $y(x, t)$ into equation (3), multiplying through by an orthogonal eigenfunction, ϕ_j, integrating over the domain, and using the equivalence

$$\int_0^L EI\phi_i'''' \phi_j\, \mathrm{d}x = \int_0^L EI\phi_i'' \phi_j''\, \mathrm{d}x = \omega_i^2 \int_0^L \rho \phi_i(x)\phi_j(x)\, \mathrm{d}x \tag{6}$$

yields

$$I_1 \ddot{\theta} + m_1 \ddot{q}_1 + 2\zeta\omega_1 \dot{q}_1 + (m_1\omega_1^2 - m_1\dot{\theta}^2)q_1 = 0, \tag{7}$$

where the term $2\zeta\omega_1\dot{q}_1$ has been added to model the internal damping of the structure.

3. NUMERICAL SIMULATION

The link was modelled as an 1 m × 5·08 cm × 0·1588 cm aluminum beam with a flexural rigidity of 1·1686 Nm^2. The model was evaluated using a Runge–Kutta fifth order method controlling the time increment step size. The relative error tolerance was held at 1×10^{-8}. A small, realistic damping factor of $\zeta = 0{\cdot}2\%$ critical was included to model energy dissipation due to the internal damping of the system. The damping due to actuator–beam interaction was also considered to be small, at $b_v = 0{\cdot}0001$. The forcing frequency was taken as 7·854.

The calculation of the amplitude probability distribution was performed as follows. First, to avoid transient effects, the first 20 000 iterations of the simulation time history were discarded. Second, the interval between the largest and smallest amplitudes of the motion was divided equally into many sub-intervals. Third, the iteration from the numerical integration was placed in the appropriate sub-interval. Fourth, the number of iterations in each sub-interval was divided by the total number of iterations. The more iterations the numerical integration has, the more accurate the distribution is. The CDF was found by taking the sum of each of the previous intervals.

4. PROBABILITY DENSITY FUNCTIONS

4.1. *PDF development*

Due to its sensitivity to the initial conditions, it is impossible to predict how a chaotic system will develop. All that can be said is that the trajectory lies somewhere on the strange attractor. The precise location of a particle in phase space cannot be known. To perform

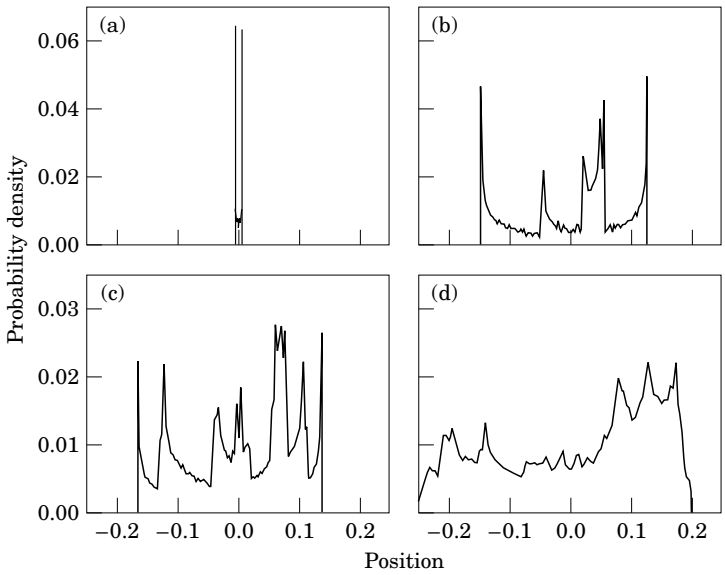

Figure 2. The position PDF of the evolution from periodic amplitude regions to chaos: (a) $A = 1{\cdot}92$; (b) $A = 1{\cdot}95$; (c) $A = 2{\cdot}06$; (d) $A = 2{\cdot}45$.

a statistical analysis of the motion it is necessary to obtain the probability of finding the particle at some point on the attractor. For an attractor there would be a corresponding probability density function (PDF) for each of the phase space co-ordinates. The PDF of a chaotic system with an attractor should also display a fractal nature, but may be hidden by experimental or computational noise.

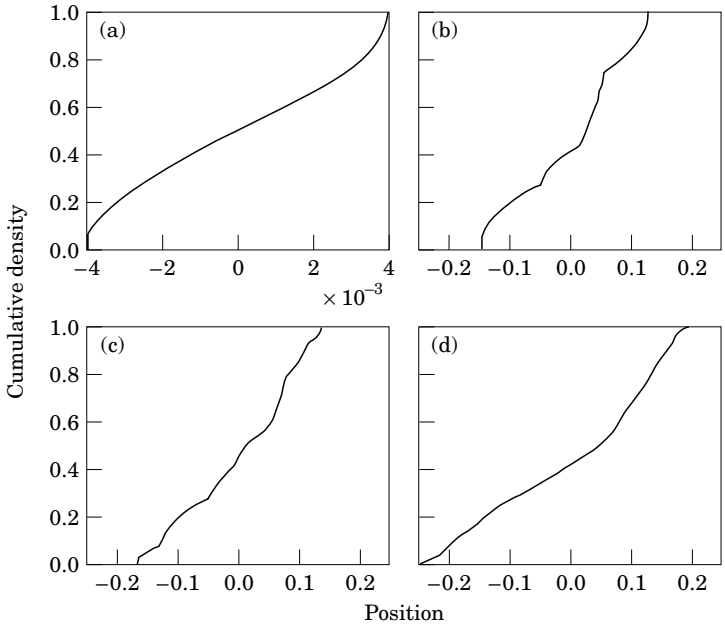

Figure 3. The position CDF of the evolution from periodic amplitude regions to chaos: (a) $A = 1{\cdot}92$; (b) $A = 1{\cdot}95$; (c) $A = 2{\cdot}06$; (d) $A = 2{\cdot}45$.

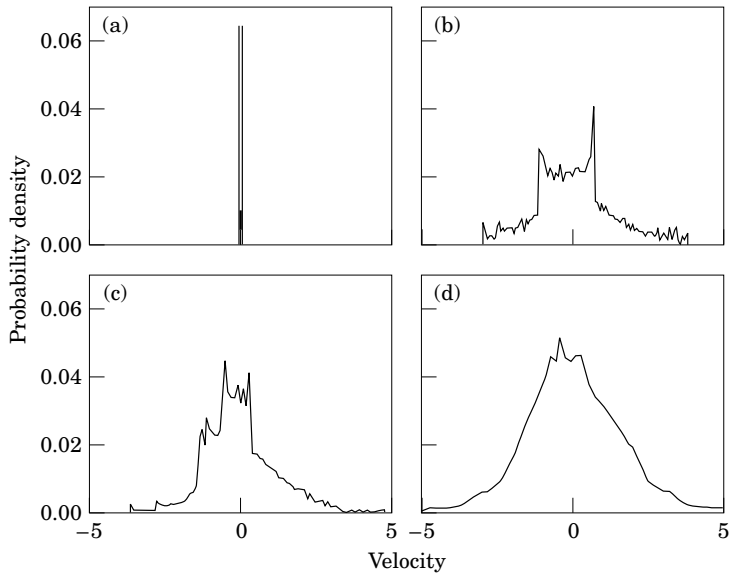

Figure 4. The velocity PDF of the evolution from periodic amplitude regions to chaos: (a) $A = 1{\cdot}92$; (b) $A = 1{\cdot}95$; (c) $A = 2{\cdot}06$; (d) $A = 2{\cdot}45$.

The evolution of the position and velocity PDFs and CDFs can be seen in Figure 2–5. The figures show the system as the forcing amplitude is increased from $A = 0{\cdot}1$ to $2{\cdot}45$. For $A = 0{\cdot}1$ the typical PDF for the linear version of this system is seen. The PDF for a periodic sequence is much different than that of a chaotic sequence. The distribution for a periodic sequence is denoted by two discrete sharp peaks at the maxima and minima,

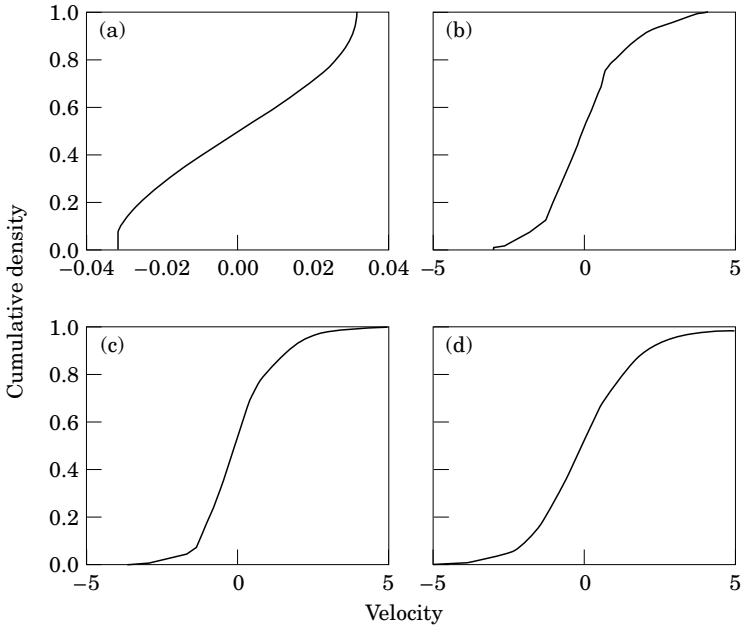

Figure 5. The velocity CDF of the evolution from periodic amplitude regions to chaos: (a) $A = 1{\cdot}92$; (b) $A = 1{\cdot}95$; (c) $A = 2{\cdot}06$; (d) $A = 2{\cdot}45$.

resulting from the elliptic nature of the limit cycle phase portrait. As the amplitude is increased the system undergoes a bifurcation which occurs at $A = 1{\cdot}92$; the system is now quasi-periodic. Increasing the amplitude results in more bifurcations until the system is continuous in its chaotic state at $A = 2{\cdot}45$. The position PDF exhibits a continuous nature and multi-maxima peaks as A increases. The velocity PDF tends towards a normal distribution but also has multi-maxima peaks. These peaks are characteristic of chaotic PDFs due to the fractal nature of the attractors.

4.2. *Multi-maxima peaks*

A chaotic system is most often described using phase portraits, correlation functions, Poincaré mappings and Lyapunov exponents. The probability density function can also be used as another criteria for a chaotic system. Unlike the PDFs of a harmonic response, which are characterized by two discrete almost maxima at the extrema (see Figures 2 and 4, $A = 0{\cdot}1$), the PDFs of a chaotic response are typically characterized by a continuous maxima diffused towards the center (see Figures 2 and 4, $A = 2{\cdot}45$) [4]. The multi-maxima peaks arise because certain amplitudes of the time series are more probable than others. This happens because, as the system is driven into its chaotic state, the strange attractor which governs the system draws points in the phase plane to it. The attractor gives a global picture of the long term behavior of the dynamical system. The PDF depends upon the length of the time series from which it is estimated.

4.3. *Sensitivity to initial conditions*

A hallmark of chaotic dynamical systems is their sensitive dependence to initial conditions. A chaotic system with two sets of almost identical initial conditions will diverge

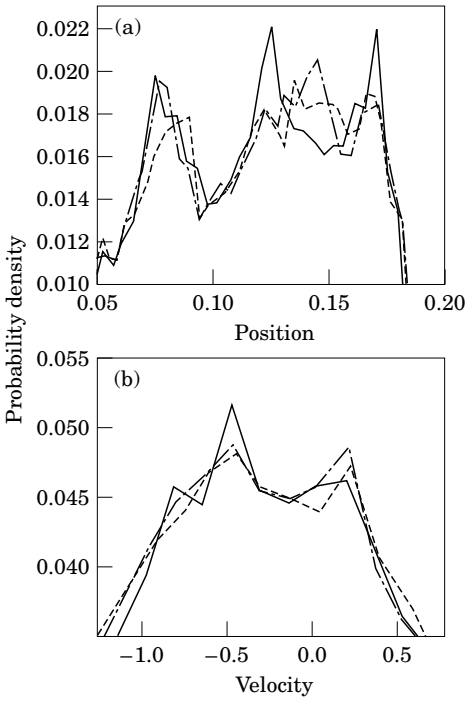

Figure 6. A PDF comparison of three initial conditions: (a) position; (b) velocity. ——, 0·01; ·····, 0·1, –·–·–, 1·0.

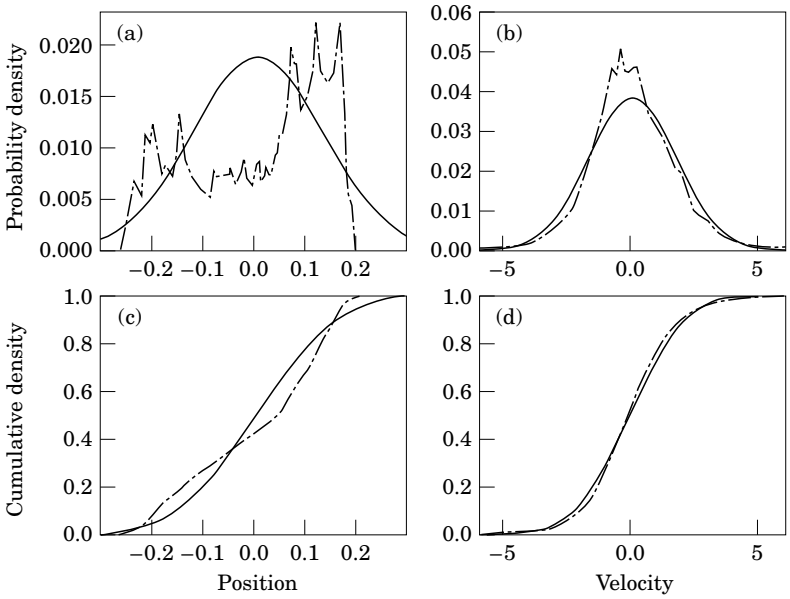

Figure 7. The normal distributions compared to the chaotic distributions: (a) position PDF versus normal PDF; (b) velocity PDF versus normal PDF; (c) position CDF versus normal CDF; (d) velocity CDF versus normal CDF.

and take on totally different trajectories after some time t. The outcome of any trial depends heavily on the starting parameters. The PDFs also show the system's sensitivity. The slewing model was evaluated at three initial end-tip displacements of 0·01, 0·1 and 1·0 with a forcing amplitude of 2·45. The position and velocity PDF results of the three can be seen in Figure 6 (where only the top portion is shown for clarity). As seen in the figure, the forms of the PDFs are similar (all are continuous and of the same general form), but they are are not identical. The CDFs (not shown) do not display the system sensitivity as readily, as expected, since they are the cumulative sum of the components.

4.4. *Comparison with normal distribution*

A comparison of the PDFs and CDFs for position and velocity was made with the normal distribution (Figure 7). A mean of 0·0044 and a standard deviation of 1·7148 were calculated from the velocity–time series data. For the position–time series data, a mean of 0·0086 and a standard deviation of 0·1297 were determined. The goodness of fit for the distributions was measured by using the chi-square and Kolmogorov–Smirnov (K–S) tests [6]. The χ^2 tests resulted in a value of 0·2138 for the position and a value of 0·05 for the velocity PDF. This would indicate that the theoretical normal distribution is acceptable at less than the 5% significance level. Thus, it would appear from this test alone that the normal curve is a valid approximation for the system's velocity distribution. The K–S test was then performed on the system. A maximum difference of $D_n = 0{\cdot}4472$ was found for the velocity distribution. For position, a maximum difference of $D_n = 0{\cdot}4565$ was found. The critical value of D_n^{α} for the distributions was calculated to be 0·128 at the 20% acceptance level. Thus, the PDFs of the system fail the K–S test in comparison to the normal distribution for anything less than 20% significance.

5. CONCLUSIONS

This investigation dealt with the identification of the characteristics of the PDF and CDF of a flexible, slewing link (as a model of a lightweight robot manipulator) as it developed from the linear region to the chaotic region. Several conclusions can be reached. As the forcing amplitude is varied, chaotic motion appears. The existence of periodic, quasi-periodic and chaotic distributions has been shown. The probability density function has distinctive features depending upon whether the system is undergoing linear or chaotic motion. The PDF of the system displays the chaoticity, while the CDF is not as good a measure. The normal distribution does not provide an adequate model of the chaotic PDF and CDF of the system as verified using the chi-square and Kolmogorov–Smirnov tests. Since the trend is to make manipulators lighter and quicker to enhance performance, care must be taken when selecting the forcing methods. The system modelled shows that chaotic motions can occur for these types of lightly damped, flexible manipulators.

REFERENCES

1. S. C. S. Yim and H. Lin 1991 *Ocean Engineering* **18**, 225. Chaotic behavior and stability of free-standing offshore equipment.
2. R. Stockton 1993 *Masters Thesis*, *Vanderbilt University*, *Nashville*, *TN*. Do links that slew, slew true? Determination of chaos of flexible structures.
3. C. Y. Yang, A. H-D. Cheng and R. V. Roy 1991 *International Journal of Probabilistic Engineering Mechanics* **6**, 193. Chaotic and stochastic dynamics for a nonlinear strurctural system with hysteresis and degradation.
4. T. Kapitaniak 1987 *Journal of Sound and Vibration* **114**, 588. Quantifying chaos with amplitude probability density function.
5. J. P. Eckmann and D. Ruelle 1987 *Review of Modern Physics* **57**, 617. Ergodic theory of chaos and strange attractors.
6. A. H-S. Ang and W. H. Tang 1975 *Probability Concepts in Engineering Planning and Design*. New York: John Wiley.